LMA: Location- and Mobility-Aware Medium-Access Control Protocols for Vehicular *Ad Hoc* Networks Using Directional Antennas

Kai-Ten Feng, *Member, IEEE*

***Abstract*—In recent years, the incorporation of the directional antennas within mobile devices has been studied in many areas. The usage of directional antennas can greatly reduce the radio interference, which results in improved utilization of the wireless medium. It becomes practical to exploit the directional antennas in the medium-access control (MAC) protocol design. In this paper, a location- and mobility-aware (LMA) MAC protocol is developed for vehicular *ad hoc* networks (VANETs). The predictive location and mobility of the vehicles are adopted to provide robust communication links while using the directional beams. The deafness problem is also alleviated using the directional-listen mechanism in the proposed algorithm. Moreover, the exploitation of the directional beacons within the scheme can enhance the reliability of the communication linkages, even when the moving directions and speeds of the vehicles have been changed. Under dynamic moving scenarios, both the spatial reuse and the routing efficiency are preserved using the proposed LMA MAC scheme. The performance of the proposed algorithm is evaluated and compared with other existing MAC protocols in simulations.**

***Index Terms*—Directional antennas, medium-access control (MAC), prediction mechanism, vehicular *ad hoc* networks (VANETs).**

I. Introduction

A MOBILE *Ad hoc* NETwork (MANET) consists of wireless Mobile Nodes (MNs) that cooperatively communicate with each other without the existence of a fixed network infrastructure. Depending on different geographical topologies, the MNs are dynamically located and continuously changing their locations. Recent interests in the design of MANET algorithms include applications for the military, the personal-communication services, the wireless-sensor networks, and the Vehicular *Ad hoc* NETworks (VANETs). The VANET [1]–[3], which can be considered as a particular type of MANET with MNs[1] (i.e., vehicles) possessing higher mobility, has attracted an increasing amount of interests in recent years. The primary concern of a VANET is to provide information exchanges for intervehicle communication (IVC), as defined in the draft of vehicle infrastructure integration [4]. By delivering messages between the MNs (e.g., safety-warning messages), the IVC system can both provide smoother driving and alleviate potential traffic accidents. However, it is difficult to achieve decentralized and multihop communication between the MNs with dynamically changing topology [5]. Moreover, the connectivity between the MNs can become unreliable due to the inherently high-mobility characteristics of the vehicles.

Different topics have been investigated in the previous work for VANETs. Conventional research studies have been devoted to medium-access control (MAC) schemes using omnidirectional antennas, e.g., the IEEE 802.11 protocol [6]. It has been studied in [7] and [8] that the omnidirectional-based medium-reservation schemes result in poor spatial utilization and link reliability. With advancements in the smart-antenna technology, it becomes feasible to consider directional antennas within the formulation of the *ad hoc* MAC protocols. Compared with the omnidirectional antenna, the benefits of using the directional antenna include spatial reuse, enlarged coverage of transmission, and enhanced network throughput [9], [10].

Many issues have been encountered in the design of the MAC protocols within MANETs, e.g., the radio interference, the switching mechanisms for antenna beams, and the deafness problem. Most current research is devoted to resolving the deafness problem, which does not happen in the MAC protocols with omnidirectional antennas. The problem happens when two MNs (A and B) are transmitting packets with their antenna beams pointing to each other directionally. A third node C, which is not located within the communication ranges of nodes A and B, attempts to deliver data packets to node A. However, node C is unaware (i.e., "deaf") of the ongoing transmission between nodes A and B due to the directional-antenna settings. Node C will continue to initiate the transmission of the Request To Send (RTS) packets to node A, which results in collision with the data packets at node A. The system performance will therefore be degraded due to the so-called deafness problem.

Manuscript received January 16, 2007; revised May 18, 2007 and July 14, 2007. This work was supported in part by the National Science Council (NSC) under Grant 92-2218-E-009-014, by the MOE ATU Program 95W803C, and by the MediaTek Research Center, National Chiao Tung University. The review of this paper was coordinated by Prof. X. Shen.

The author is with the Department of Communication Engineering, National Chiao Tung University, Hsinchu 300, Taiwan, R.O.C. (e-mail: ktfeng@mail.nctu.edu.tw).

Digital Object Identifier 10.1109/TVT.2007.906874

[1]In this context, "vehicle" is denoted as "MN" for generic purposes.

With the prosperity of vehicles equipped with positioning systems (such as global positioning systems (GPSs) [11]), it becomes feasible for each vehicle to obtain its own position and velocity information from its upper network layer protocols for the design of the MAC algorithm. The potential movement between the MNs has not been taken into consideration in previous directional-antenna-based MAC algorithms. Under the dynamic movement between the MNs, the communication linkages may become fragile and unreliable. In this paper, the proposed location- and mobility-aware (LMA) MAC scheme considers the relative movement between the MNs within the design of the directional-antenna-based MAC algorithm. The antenna beams of both MNs during data transmission are adjusted based on their predicted locations. Moreover, the deafness problem is improved by adapting a switching mechanism based on the information stored in the location table of each MN. Either an Omni-Listen/Omni-RTS [O-Listen/O-RTS (OLR)] or a Directional-Listen/Directional-RTS [D-Listen/D-RTS (DLR)] pair is utilized for each MN to initiate a new data transmission. The usage of the directional-beacon (DB) mechanism within the proposed scheme can facilitate the MNs to always obtain the correct position and mobility information after one node has changed its moving direction or velocity. The robustness of the communication linkages can therefore be preserved. Within the directional-antenna-based VANETs, the proposed LMA MAC scheme alleviates both of the following: 1) the deafness problem and 2) the unreliable communication linkages under dynamic moving scenarios. The performance comparison between the proposed algorithm and other existing MAC protocols will be evaluated via simulations.

The rest of this paper is organized as follows. Section II reviews the related *ad hoc* MAC protocols, including brief summaries of the existing IEEE 802.11 and the directional MAC (DMAC) algorithms. The proposed LMA MAC protocol is described in Section III. The computation of the Out-of-Range Predictors (ORPs) for both the LMA MAC and the DMAC schemes are presented in Section IV. The performance evaluation and comparison of the proposed LMA MAC algorithm, with the associated simulation parameters, are shown in Section V. Section VI draws the conclusions.

II. Related Work

Different types of directional-antenna-based MAC protocols have been proposed [12]–[15], [17], [18], [21]–[31]. Conventional studies on the usage of the directional antennas have been focused on the protocol design in broadband and cellular networks [12], [13]. Earlier work [14], [15] on directional-antenna-based MANETs proposed conservative MAC schemes using O-RTS/Clear To Send (CTS) control packets, whereas the data packets are transmitted using directional beams. The primary drawback is that the transmission range and spatial reuse are limited due to the use of omnidirectional control packets [16]. A proactive approach is proposed in [17] by distributing the MNs' traffic pattern to its neighborhood. However, excessive control packets are encountered in this proactive scheme. The DMAC/multihop MAC (MMAC) approaches developed in [18] utilizes the directional beams for transmitting both the control and the data packets. The two major drawbacks of these approaches include the following: 1) the prerequisite for each MN to be aware of all the MNs' location information in the network and 2) the unsolved hidden terminal [19] and deafness problems [20]. The circular RTS MAC protocol proposed in [21] partially resolved the problems in the DMAC/MMAC algorithms. However, a large amount of RTS packets are required to accomplish the circular rotation of the antenna beams.

The hidden-terminal problem is improved by using a busy-tone channel, as proposed in [22] and [23]. The additional assignment of control channel is required in these schemes with the unsolved deafness problem. Recent works to reveal and describe the deafness problem have been studied in [20] and [24]. Two preliminary MAC schemes were proposed in [24] to proactively alleviate the problem. The ToneDMAC [25] and the smart-antenna-based wide-range-access MAC [26] protocols conquer the deafness problem by incorporating either an additional control channel or a start-of-frame in the protocol design. The scheme proposed in [27] combines a directional network-allocation vector (DNAV) indicator and an orthogonal routing mechanism to improve the deafness problem. The DNAV, as adopted in [14], [18]–[21], and [28], utilizes the concept of directional virtual carrier sensing to alleviate collisions with packets. It is noted that the DNAV represents a table that prohibits the corresponding MN to initiate data transmission along the direction of an ongoing packet transmission. The DMAC with deafness-avoidance and collision-avoidance protocol proposed in [29] also revealed that the deafness problem has much greater impact on network performance compared with that from the hidden-terminal problem.

Moreover, a few research studies have been dedicated to the power-control mechanisms for directional-antenna-based *ad hoc* networks. An integrated model for analyzing the smart-antenna-based MANET has been proposed in [30]. The appropriate power levels for both the control and data packets are determined as in [30] and [31], which are studied to be influential on the spatial reuse of the networks. In order to facilitate the design of the proposed LMA MAC scheme, two conventional MAC algorithms, including the IEEE 802.11 and the DMAC protocols, are briefly summarized as follows.

A. IEEE 802.11 Protocol

The IEEE 802.11 is standardized based on the omnidirectional antenna. The distributed coordination function (DCF) is the basic access mechanism utilized in the IEEE 802.11 MAC protocol [6]. The DCF is based on the carrier-sensing multiple access with a collision-avoidance scheme to ensure that each MN gets a fair chance to access the wireless medium. In order to avoid data collision within the medium, the virtual carrier-sensing mechanism, which is carried out by the NAV, is utilized to record the duration of the ongoing data transmission. A random backoff process is also executed in each MN to decrease the probability of data collision. Moreover, the optional RTS/CTS exchange before the data transmission is exploited to resolve the potential hidden-terminal problem.

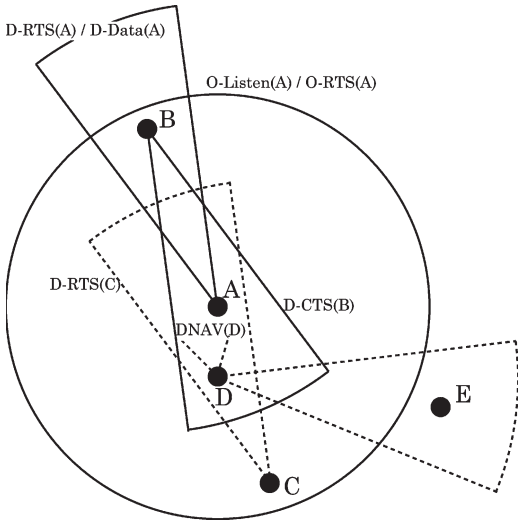

Fig. 1. Schematic diagram for the DMAC and the proposed LMA MAC schemes.

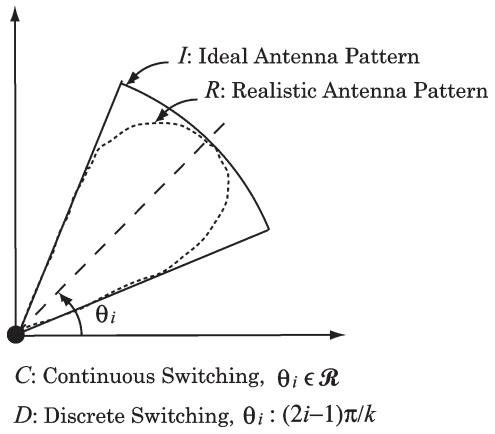

Fig. 2. Schematic diagram for various antenna switching mechanisms and patterns.

B. DMAC Protocol

The DMAC scheme [18] is one of the well-known directional-antenna-based MAC protocols. Each MN is assumed to possess the position information of all the MNs in the network. While in the idle state, the MNs are listening to the medium in the omnidirectional mode (O-Listen). Fig. 1 shows that node A is listening to the omnidirectional mode, i.e., O-Listen(A). The MNs' antenna is switched to the directional mode while it is sending either the control or the data packets. After the D-RTS/Directional-CTS (D-RTS/D-CTS) exchange has been completed [e.g., D-RTS(A)/D-CTS(B) as in Fig. 1], the Directional-Data/Directional-Data-Acknowledgement (D-Data/D-Data-ACK) can therefore be accomplished. Upon receiving either the D-RTS(A) or D-CTS(B) control packet, the MNs, other than the transmission pair A and B, will update their NAV directionally, e.g., the DNAV(D) by node D, as in Fig. 1. Comparing with traditional omnidirectional-based MAC algorithms, the DMAC protocol increases the spatial reuse in MANETs. However, it suffers from the problem of deafness. As shown in Fig. 1, node C is unaware of the ongoing transmission between nodes A and B due the unheard D-RTS(A)/D-CTS(B) exchange. In the case that node C intends to transmit data packets to node A, it will transmit the D-RTS(C) packet toward node A. A collision will occur at node A with the continuous retransmission of the D-RTS(C) packets.

III. Proposed LMA MAC Protocol

The following assumptions are served as the prerequisites for the proposed LMA MAC scheme.

1) The location information of each MN, including position, velocity, and moving angle, is assumed to be obtainable from its upper network layer.
2) All the MNs within the network are moving at constant speeds within a short period of time, i.e., the packet exchanges considered in the LMA MAC scheme are conducted with the MNs possessing constant velocities and moving angles. However, this assumption becomes optional after the incorporation of the DB within the LMA MAC algorithm, which will be discussed in Section III-C.
3) The types of directional antenna utilized in the proposed LMA MAC scheme can be classified based on their switching mechanisms and the antenna patterns [32], [33], as shown in Fig. 2. There are four different cases considered in this paper.
   a) CI $= \{\theta_i, p \mid 0 \le \theta_i < 2\pi, \theta_i, i \in \Re, p \in \mathcal{I}\}$.
   b) CR $= \{\theta_i, p \mid 0 \le \theta_i < 2\pi, \theta_i, i \in \Re, p \in \mathcal{R}\}$.
   c) DI $= \{(\theta_i, p) \mid \theta_i = (2i-1)\pi/k, \theta_i \in \Re, i = 1, \ldots, k, p \in \mathcal{I}\}$.
   d) DR $= \{(\theta_i, p) \mid \theta_i = (2i-1)\pi/k, \theta_i \in \Re, i = 1, \ldots, k, p \in \mathcal{R}\}$.

   The two parameters (θ_i, p) within the four cases denote the antenna rotating angle and the antenna pattern. Case a) represents the situation with the Continuous (C) switching antenna (i.e., steerable adaptive array antennas) with the Ideal (I) antenna pattern. The main lobe of the antenna is directed to the MN of interest in order to maximize the antenna gain. The configuration of the ideal antenna pattern $(\mathcal{I})$ denotes that the antenna is associated with sector shape (as in Fig. 2), i.e., the same antenna gain for both the main lobe and the sidelobes. The two parameters (θ_i, p) associated with the CI case indicate that the antenna has continuous switching angle (i.e., $\theta_i \in \Re$, $0 \le \theta_i < 2\pi$) and ideal pattern $(p \in \mathcal{I})$. On the other hand, case d) indicates the setting with the discrete (D) switching antenna (i.e., switched-beam or fixed-beam antennas) with a realistic (R) antenna pattern. The main lobe of the antenna is pointed at the prespecified directions based on the number of sectors [i.e., the parameter k as in case d)]. For example, if k equals four, the parameters $\theta_1 = \pi/4$, $\theta_2 = 3\pi/4$, $\theta_3 = 5\pi/4$, and $\theta_4 = 7\pi/4$. The configuration of the realistic antenna pattern $(\mathcal{R})$ indicates that the antenna gains associated with the sidelobes are comparably smaller than that with the main lobe of the antenna (as in Fig. 2). Case b), with continuous switching and realistic antenna pattern (CR), and case c), with discrete switching and ideal antenna pattern (DI), can also be justified similarly. The proposed LMA MAC

scheme will be explained and analyzed using the first case (i.e., the CI case with continuous switching and ideal antenna pattern). The remaining three cases will also be considered and implemented in the simulation section for performance comparison.

The proposed LMA MAC protocol utilizes the RTS and the CTS control packets for the MN to transport its location information to the neighborhood MNs. The location information is stored in the location table (LT) in each MN, where the format of the ith entry of the LT $= \{\text{LT}(i)|1 \le i \le n\}$ can be represented as

$$\text{LT}(i) = \langle \text{TimeStamp, NodeID, Position, MovingAngle, Velocity, } \Delta T^{\text{LMA}} \rangle \quad (1)$$

where TimeStamp represents the time instant that the information for the corresponding MN is stored in the LT(i). It is worthwhile to indicate that ΔT^{LMA} is served as an ORP for the proposed LMA algorithm, which is utilized to imply the effectiveness of this LT(i) entry. The ORP represents the time interval that the MN recorded in the LT(i) entry will stay within the transmission range of the MN that possesses this LT. The value of ΔT^{LMA} is calculated based on the relative distance and velocity between the two MNs in consideration. The exact computation of the ΔT^{LMA} value will be explained and acquired in Section IV. The value of ΔT^{LMA} will be decremented as time elapsed. As ΔT^{LMA} goes to zero, the associated LT(i) entry is removed from the MNs' LT. It corresponds to the situation that the MN, as recorded within the LT(i) entry, travels out of the transmission range of the MN in consideration. The values of the parameters associated within this LT(i) entry are no longer valid.

Based on the available information acquired from a MN's LT, the MN can adjust itself into either the OLR or the DLR mode. The proposed LMA MAC scheme with the two transmission modes is described in Sections III-A and B. It will also be observed in Section III-B that the deafness problem resulting from the directional antenna can be alleviated by using the DLR mode. The incorporation of the DB within the proposed scheme will be addressed in Section III-C.

A. OLR Mode

Figs. 1 and 3 show the schematic and the timing diagrams of the proposed LMA MAC scheme. The solid lines (as in Fig. 3) associated with nodes A, B, and C indicate the timelines and the moving directions of these three MNs. In the case that node A intends to deliver data packets to node B, it will conduct the default O-Listen(A) mode to its neighborhood MNs, since node A does not have any prior location information about node B in its LT$_A$. After channel contention, an O-RTS$(A(t_r))$ packet initiated by A will be delivered omnidirectionally to node A's neighborhood MNs. It is noticed that the O-RTS$(A(t_r))$ packet contains location information of node A, including the current time stamp (t_r), the current position $(P_A(t_r) = (x_A(t_r), y_A(t_r)))$, the moving angle $(\alpha_A(t_r))$, and the velocity $(V_A(t_r))$. The neighborhood MNs of A (including the desirable delivering node B and the other nodes C and D,

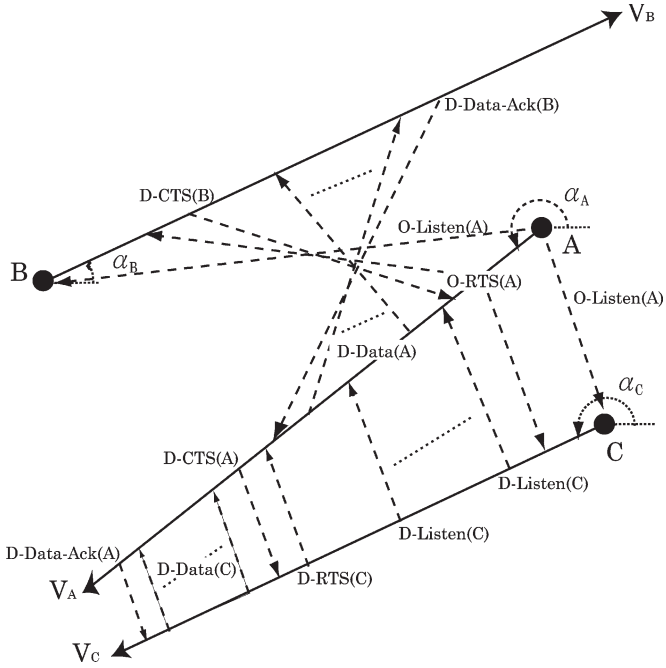

Fig. 3. Timing diagram of the proposed LMA MAC scheme.

as in Fig. 1) will record node A's location information in their LT's while omnidirectionally listening to the O-RTS$(A(t_r))$ packet in their idle states. For instance, after receiving the O-RTS$(A(t_r))$ packet from node A, an entry in the location table of B (LT$_B$) will be updated as

$$\text{LT}_B(A) = \left\langle t_r, ID_A, P_A(t_r), \alpha_A(t_r), V_A(t_r), \Delta T_A^{\text{LMA}}(t_r) \right\rangle \quad (2)$$

where $\Delta T_A^{\text{LMA}}(t_r)$ is computed as the time interval for node A to travel outside of the transmission range of node B based on their relative configuration at time t_r. To acknowledge the O-RTS$(A(t_r))$ request from node A, a D-CTS$(B(t_c))$ packet will be sent at time t_c from node B to A after channel contention. The D-CTS packet is delivered along the $\theta_{\text{cts}}^{AB}(t_c)$ direction, which can be obtained as

$$\theta_{\text{cts}}^{AB}(t_c) = \tan^{-1} \frac{y_B(t_c) - y_A(t_c)}{x_B(t_c) - x_A(t_c)} \quad (3)$$

where $P_B(t_c) = (x_B(t_c), y_B(t_c))$ represents node B's position acquired at the time instant t_c. The position of node A at time $t_c(P_A(t_c))$ can be computed at node B as

$$x_A(t_c) = x_A(t_r) + V_A(t_r) \cos \alpha_A(t_r) \cdot (t_c - t_r) \quad (4)$$

$$y_A(t_c) = y_A(t_r) + V_A(t_r) \sin \alpha_A(t_r) \cdot (t_c - t_r) \quad (5)$$

where $P_A(x_A(t_r), y_A(t_r))$, $V_A(t_r)$, and $\alpha_A(t_r)$ are obtainable from node B's LT$_B(A)$, as in (2). With the transmission of the D-CTS$(B(t_c))$ packet, the location information of node B is also delivered to node A. An entry in the location table of A is updated as

$$\text{LT}_A(B) = \left\langle t_c, ID_B, P_B(t_c), \alpha_B(t_c), V_B(t_c), \Delta T_B^{\text{LMA}}(t_c) \right\rangle. \quad (6)$$

The intended transmission of data packets from node A to B will be sent at time t_d after the O-RTS($A(t_r)$)/D-CTS($B(t_c)$) exchange. Both nodes A and B adjust their main antenna beam by pointing along the direction of $\theta^{AB}_{\text{data}}(t_k)$ for data transmission. The angle $\theta^{AB}_{\text{data}}(t_k)$ is obtained as

$$\theta^{AB}_{\text{data}}(t_k) = \tan^{-1}\frac{y_A(t_k) - y_B(t_k)}{x_A(t_k) - x_B(t_k)} \tag{7}$$

where $t_k = \{t \in \Re | t_d \le t \le t_s\}$ represents the time instant which falls between the starting (t_d) and the stopping (t_s) time instants for data transmission. The positions of nodes A and B at the time instant t_k can also be computed as

$$\begin{aligned} P_A(t_k) &= (x_A(t_k), y_A(t_k)) \\ &= (x_A(t_r) + V_A(t_r)\cos\alpha_A(t_r)\cdot(t_k - t_r)y_A(t_r) \\ &\quad + V_A(t_r)\sin\alpha_A(t_r)\cdot(t_k - t_r)) \end{aligned} \tag{8}$$

$$\begin{aligned} P_B(t_k) &= (x_B(t_k), y_B(t_k)) \\ &= (x_B(t_c) + V_B(t_c)\cos\alpha_B(t_c)\cdot(t_k - t_c)y_B(t_c) \\ &\quad + V_B(t_c)\sin\alpha_B(t_c)\cdot(t_k - t_c)) \end{aligned} \tag{9}$$

where $P_A(t_k)$ is computed at node B based on the information in the $\text{LT}_B(A)$, as in (2); $P_B(t_k)$ is calculated at node A from its $\text{LT}_A(B)$, as in (6). It is noticed that the angle $\theta^{AB}_{\text{data}}(t_k)$ is a time-varying and incrementally changing parameter as the MNs are dynamically moving. The angle $\theta^{AB}_{\text{data}}(t_k)$ can be adjusted in a continuous or a discrete manner, depending on the configuration of the antenna in the MNs, as shown in Fig. 2. After the data transmission is completed, the associated D-Data-ACK($B(t_a)$) will be issued by node B at time t_a in the directional manner based on the relative position between nodes A and B.

Moreover, node D set its DNAV(D) after receiving the D-CTS($B(t_c)$) from node B, as shown in Fig. 1. Node D will not be able to conduct packet transmission within the confined range that is set by the DNAV(D). However, node D can still transmit data packets that are exterior to the DNAV(D) region if it possess the location information of its intended destination node within the LT_D. The details will be explained in the next section.

B. DLR Mode

The DLR mode of the proposed LMA MAC protocol is primarily utilized to resolve the problem of deafness coming from the directional-antenna-based configuration. Without any prior information, the MNs within the network stay in the O-Listen mode while in the idle state. In the case of a new data transmission between two MNs, the sender can exploit the location information from its previously stored LT(i) to predict the position of its intended destination node. The antenna beam of the sender will be directed to the predicted direction of the destination node in order to initiate the D-Listen mode.

As shown in Fig. 3, node C obtains the location information of node A by listening to the O-RTS($A(t_r)$) packet, which is targeted to node B, as described in the previous section. After receiving the O-RTS($A(t_r)$) packet from node A, an entry within the location table of C is updated as $\text{LT}_C(A)$, which is the same as $\text{LT}_B(A)$ [in (2)] recorded in node B. There can be possibility that node C also intends to send data packets to node A during the transmission between nodes A and B. As shown in Fig. 3, node C will conduct D-Listen(C) toward the direction of node A's location, where the current position of node A is calculated from the $\text{LT}_C(A)$ entry. The transmission medium within the range confined by D-Listen(C) mode may still be busy due to the ongoing packet delivery between nodes A and B. Node C will continue to listen to node A directionally using the D-Listen(C) mode, as in Fig. 3. It is also noted that the relative angle between nodes A and C may change as time progresses. Node C will be responsible for calculating its transmission angle to node A, which is similar to the computation in (7)–(9).

The following situations can happen after the completion of the data transmission between nodes A and B. Node C may travel out of the transmission range of node A, which is indicated by an expired $\text{LT}_C(A)$ entry with $\Delta T^{\text{LMA}}_A = 0$. In this case, node C will restart its original OLR mode for data transmission toward node A. On the other hand, node C will sense that the medium becomes free by using its D-Listen(C) mode associated with a valid ΔT^{LMA}_A value within its $\text{LT}_C(A)$ entry. After the random backoff time, node C will initiate a D-RTS packet, i.e., D-RTS($C(t'_r)$), to node A at the time instant t'_r to request for data delivery. The transmission angle $(\theta^{CA}_{\text{rts}})$ from node C to node A can be obtained as

$$\theta^{CA}_{\text{rts}} = \tan^{-1}\frac{y_C(t'_r) - y_A(t'_r)}{x_C(t'_r) - x_A(t'_r)} \tag{10}$$

where the position of node A at time t'_r can be computed at node C from the $\text{LT}_C(A)$ as

$$x_A(t'_r) = x_A(t_r) + V_A(t_r)\cos\alpha_A(t_r)\cdot(t'_r - t_r) \tag{11}$$

$$y_A(t'_r) = y_A(t_r) + V_A(t_r)\sin\alpha_A(t_r)\cdot(t'_r - t_r). \tag{12}$$

The remaining processes for achieving the data transmission from node C to A [i.e., D-CTS(A), D-Data(C), and D-Data-ACK(A)] will follow the similar procedures, as described in the previous section, by adopting the OLR mode.

The DLR mode is also beneficial for spatial reuse. It allows the MNs to initiate a new data delivery, albeit they are within the range of an ongoing data transmission. As indicated in the previous section, node D sets its DNAV(D) along the direction where nodes A and B are conducting data transmission. In the case that node D intends to transmit data packets to node E, which is assumed not in the DNAV(D) region, as shown in Fig. 1, node D will verify if it possesses a table entry $\text{LT}_D(E)$ with a nonzero ΔT^{LMA}_E value. If the corresponding conditions are satisfied, node D will conduct D-Listen(D) mode toward the direction of node E. If the transmission medium is found to be free, the associated D-RTS(D), D-CTS(E), D-Data(D), and D-Data-ACK(E) will be performed based on the computation as described before. In order to consider the dynamic-changing

networks, the direction of the DNAV associated with each MN is designed to be adaptable based on the mobility of the related neighborhood MNs. Since node D has recorded the location information of both nodes A and B in its location table (i.e., the table entries $\mathrm{LT}_D(A)$ and $\mathrm{LT}_D(B)$), the DNAV(D) can therefore be adjusted based on the movement of these two nodes.

Furthermore, node C may terminate its D-Listen(C) mode toward node A after a period of time due to the ongoing transmission between nodes A and B. In the case where node C intends to transmit packets to node E without the knowledge of data transmission between nodes D and E, node C will initiate either one as follows: 1) the default O-Listen(C) mode while the table entry $\mathrm{LT}_C(E)$ does not exist in its location table or 2) the D-Listen(C) toward node E with the existence of the $\mathrm{LT}_C(E)$ entry. Node C will continue the listening process until the transmission between nodes D and E has been terminated, which prevents the potential packet collision that may happen at node E.

C. Adoption of the DB

As mentioned at the beginning of this section, the proposed LMA MAC protocol is valid based on the assumption that the MNs move at constant speeds within the handshaking cycle for data transmission. In certain occasions, however, the MNs may change their speeds or moving angles during the transmission of the control or data packets. The proposed LMA MAC algorithm could result in inaccurate prediction of the MNs' movements. In this section, an additional mechanism, i.e., the DB, is exploited to alleviate this problem.

As shown in Fig. 3, the antenna beams of nodes A and B are pointed to the predicted directions based on the LMA MAC algorithm. Both MNs can successfully conduct the handshaking cycle for data delivery under the assumption of constant moving speeds, i.e., V_A, V_B, α_A, and α_B are constant values within the transmission time interval. However, the constant-speed scenario does not happen all the time. The moving angle and velocity of the MN can be varied during the transmission of the data packets. Moreover, the location-prediction mechanism within the DLR mode may fail if the moving angles or speeds that are changed between the MNs are considered. As shown in Fig. 3, node C utilizes the D-Listen(C) mode toward node A to request for potential data transmission to node A at a later time. In the case that node A adjusts its moving behaviors during the time interval of D-Listen(C), node C may not succeed to direct its antenna beam to node A with the location prediction based on its original $\mathrm{LT}_C(A)$ table entry.

In order to improve the problem of incorrect location prediction, the DB is utilized as an assisted mechanism for the LMA MAC protocol. As shown in Fig. 4, node B varies its velocity and moving angle at time t_{db} from V_B and α_B to V_B' and α_B'. It is noted that the mobility-changing information was acquired from node B's upper layer protocols. A DB will be initiated by node B toward the direction that was originally calculated for data transmission, i.e., directed to node A, as shown in Fig. 4. The updated mobility information of node B will be delivered via the DB to its neighborhood MNs (e.g., node A) within the transmission range. The $\mathrm{LT}_A(B)$ entry in the LT_A, which was formerly assigned in (6), will be updated as

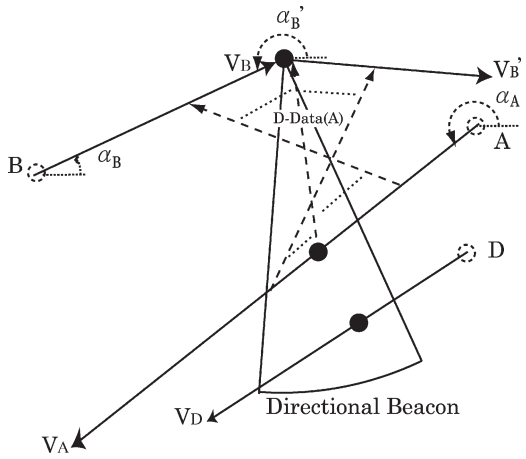

Fig. 4. Timing diagram of the proposed LMA MAC scheme with the DB.

$$\mathrm{LT}_A(B) = \langle t_{\mathrm{db}}, ID_B, P_B(t_{\mathrm{db}}), \alpha_B(t_{\mathrm{db}}), V_B(t_{\mathrm{db}}), \Delta T_B^{\mathrm{LMA}}(t_{\mathrm{db}}) \rangle \quad (13)$$

where $\alpha_B(t_{\mathrm{db}}) = \alpha_B'$, and $V_B(t_{\mathrm{db}}) = V_B'$. The $\Delta T_B^{\mathrm{LMA}}(t_{\mathrm{db}})$ value is recomputed to represent the renewed lifetime of this $\mathrm{LT}_A(B)$ entry, i.e., the updated time interval for node A to leave the transmission range of node B. The relative transmission angle $\theta_{\mathrm{data}}^{AB}(t_k)$ [as in (7)] will therefore be recalculated by node A based on the updated information obtained from the $\mathrm{LT}_A(B)$ entry. It is noticed that the other neighborhood MNs (within the transmission range of node B) will also acquire the location information via the DB transmitted by node B. For example, as shown in Fig. 4, node D will also update an entry in its LT_D as $\mathrm{LT}_D(B) = \mathrm{LT}_A(B)$, which is the same as defined in (13). In the case of potential data transmission between nodes B and D, the updated information existed in the $\mathrm{LT}_D(B)$ entry will assist node D to provide a more precise location prediction of node B. The performance evaluation of the proposed LMA MAC scheme (with and without the exploitation of the DB mechanism) will be evaluated in the simulation section.

IV. Computation of the ORP

The ORP is utilized to represent the predicted time interval before two MNs moving out of the transmission range between each other. The ORP value, which is adopted within the location table of the LMA MAC scheme [as in (1)], is served as an indicator to describe the time interval that two MNs can communicate using the directional-antenna configuration. As shown in Fig. 5, the two nodes A and B are assumed to be located at $P_A(t_0) = (x_A(t_0), y_A(t_0))$ and $P_B(t_0) = (x_B(t_0), y_B(t_0))$ with their moving angles and velocities as $\alpha_A(t_0)$, $\alpha_B(t_0)$, $V_A(t_0)$, and $V_B(t_0)$, where t_0 represents the initial time instant for computation. The relative distance d and angle θ can be obtained as $d(t_0) = \{[x_B(t_0) - x_A(t_0)]^2 + [y_B(t_0) - y_A(t_0)]^2\}^{1/2}$ and $\theta(t_0) = \tan^{-1}(y_B(t_0) - y_A(t_0)/x_B(t_0) - x_A(t_0))$. As mentioned previously in assumption (3) in Section III, the CI case (i.e., the continuous beam switching

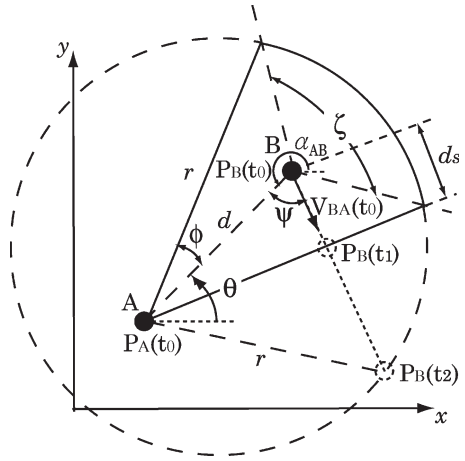

Fig. 5. Schematic diagram for the computation of the ORP.

with ideal antenna pattern) is assumed for the ORP computation. The directional beam of node A is pointed to node B with the center of its main lobe. The ideal pattern (i.e., the sector shape) of the directional antenna spans with the angle of ϕ along both sides. The transmission range of the MN is assumed to be r.

In the following sections, the calculation of the ORP value for the proposed LMA MAC scheme (i.e., ΔT^{LMA}) will be performed in Section IV-A, whereas the value of the ORP using the DMAC algorithm (denoted as ΔT^{DMAC}) will also be computed in Section IV-B. It is noted that there is no such ΔT^{DMAC} value utilized in the DMAC algorithm for out-of-range prediction. The purpose in computing this value is to illustrate the difference between these two ORP values, i.e., one is associated with the prediction mechanism of the LMA MAC scheme (i.e., ΔT^{LMA}), and the other is not (i.e., ΔT^{DMAC}). The comparison of the two ORP values adopted by these two algorithms will be analyzed and evaluated in the simulation section.

A. Computation of ORP for the LMA MAC Scheme

The ORP value for the LMA MAC scheme is computed in this section. The benefits acquired from the proposed LMA MAC protocol (associated with the DB mechanism) will be revealed. Without loss of generality, node A is assumed to be stationary at time t_0 while the resulting moving angle and velocity of node B become $\alpha_{BA}(t_0) = \alpha_B(t_0) - \alpha_A(t_0)$ and $\vec{V}_{BA}(t_0) = (V_{BA,x}(t_0), V_{BA,y}(t_0)) = (V_B(t_0) \cdot \cos\alpha_B(t_0) - V_A(t_0) \cdot \cos\alpha_A(t_0), V_B(t_0) \cdot \sin\alpha_B(t_0) - V_A(t_0) \cdot \sin\alpha_A(t_0))$. The position of node B at time t_i (for $t_i = \{t \in \Re | t \geq t_0\}$) can be represented as

$$\begin{aligned} P_B(t_i) &= (x_B(t_i), y_B(t_i)) \\ &= (x_B(t_0) + V_{BA,x}(t_0) \cdot (t_i - t_0), y_B(t_0) \\ &\quad + V_{BA,y}(t_0) \cdot (t_i - t_0)) . \end{aligned} \tag{14}$$

As described in the LMA MAC scheme, the location information between nodes A and B can be exchanged under the following conditions: 1) While both MNs are moving at constant speeds, the location information are exchanged via the RTS/CTS handshaking [as was recorded in the $\mathrm{LT}_B(A)$ in (2) and the $\mathrm{LT}_A(B)$ in (6)], and 2) while the speeds of the MNs are changed during data transmission, the location information of the MNs are delivered via the DB mechanism [as in the $\mathrm{LT}_A(B)$ in (13)]. As a result, the initial time instant t_0 for acquiring the position of nodes A and B (i.e., $P_A(t_0)$ and $P_B(t_0)$ as in Fig. 5) corresponds to either t_r, t_c, or t_{db}, depending on the different scenarios that may occur. Both MNs can conduct packet transmission starting from the time instant t_0. As the LMA MAC scheme associated with the DB mechanism is adopted, node B will still be able to communicate with node A after $t_i > t_1$. Node A will change the direction of its antenna beam in order to accommodate the changing mobility of node B during transmission. The time interval for mutual communication can be elongated until $t_i = t_2$, which indicates that node B is located at the farthest distance from node A (i.e., $P_B(t_2)$) before they are out of their transmission ranges. Therefore, the time interval from the current location update to the time that node B will be out of the transmission range of node A becomes $\Delta T_i^{\mathrm{LMA}} = t_2 - t_0$. As shown in Fig. 5, the distance between nodes A and B at time t_2 will be equal to the transmission range r as

$$r = \|P_B(t_2) - P_A(t_2)\| = \|P_B(t_2) - P_A(t_0)\| \tag{15}$$

since node A is considered stationary. By substituting (14) into (15), the ORP value, i.e., ΔT^{LMA}, can be obtained as

$$\begin{aligned} \Delta T^{\mathrm{LMA}}(t_0) &= (t_2 - t_0) \\ &= \frac{1}{V_{BA}^2(t_0)} \Big\{ \left[V_{BA}^2(t_0) \cdot \left(r^2 - d^2(t_0)\right) \right. \\ &\quad \left. + \kappa^2(t_0) \right]^{1/2} - \kappa(t_0) \Big\} \end{aligned} \tag{16}$$

where $\kappa(t_0) = V_{BA,x}(t_0) \cdot (x_B(t_0) - x_A(t_0)) + V_{BA,y}(t_0) \cdot (y_B(t_0) - y_A(t_0))$. The $\Delta T^{\mathrm{LMA}}(t_0)$, as in (16), will be utilized as a predictor in the LMA MAC scheme to determine the lifetime of its corresponding table entry.

B. Computation of ORP for the DMAC Scheme

Without the exploitation of the proposed LMA MAC scheme, the antenna beam of node A will not be adaptable based on the changing movement of node B. Both MNs will be out of their communication ranges if node B travels beyond the time instant t_1, i.e., $t_i > t_1$. Two different cases need to be considered in order to compute the ΔT^{DMAC} value. As shown in Fig. 5, the angle ζ is computed in distinguishing these two cases as

$$\zeta(t_0) = 2\tan^{-1}\left(\frac{r \cdot \sin\phi}{r \cdot \cos\phi - d(t_0)}\right). \tag{17}$$

The two cases are discussed as follows:

Case 1) This case corresponds to the situation in which the relative moving angle $\alpha_{BA}(t_0)$ between nodes A and B falls within the range of $\theta(t_0) - (\zeta(t_0)/2) \leq \alpha_{BA}(t_0) < \theta(t_0) + (\zeta(t_0)/2)$, i.e., node B is traveling out of the transmission range of node A

toward the arc of the sector shape. The resulting ORP value will be the same as that derived in the previous section as (16), i.e.,

$$\Delta T^{\mathrm{DMAC},I}(t_0) = \Delta T^{\mathrm{LMA}}(t_0). \quad (18)$$

Case 2) In this case, the relative moving angle $\alpha_{BA}(t_0)$ falls within the range of $\theta(t_0) + (\zeta(t_0)/2) \leq \alpha_{BA}(t_0) < 2\pi + \theta(t_0) - (\zeta(t_0)/2)$, i.e., node B is moving along one of the sides of the sector shape. As shown in Fig. 5, the longest distance for node B to travel will be equal to $d_s(t_0)$, i.e., up to the time instant t_1. The time interval $\Delta T^{\mathrm{DMAC,II}} = t_1 - t_0$ can be computed by using the Law of Sines as

$$\Delta T^{\mathrm{DMAC,II}}(t_0) = \frac{d_s(t_0)}{|V_{BA}(t_0)|} = \left| \frac{d(t_0) \cdot \sin\phi}{V_{BA}(t_0) \cdot \sin(2\pi - \phi - \psi(t_0))} \right| \quad (19)$$

where $\psi(t_0) = |\bmod(\theta(t_0) + \pi) - \alpha_{BA}(t_0)|$ and $\bmod(\cdot)$ indicate the modulus of the value being considered. By combining both cases, the ORP value for the DMAC scheme can be obtained from (18) and (19) as

$$\Delta T^{\mathrm{DMAC}}(t_0) = P_r(\zeta) \cdot \Delta T^{\mathrm{DMAC,I}}(t_0) + P_r(2\pi - \zeta) \cdot \Delta T^{\mathrm{DMAC,II}}(t_0) \quad (20)$$

where $P_r(\zeta) = (\zeta(t_0)/2\pi)$ and $P_r(2\pi - \zeta) = 1 - (\zeta(t_0)/2\pi)$ represent the probabilities for either case 1) or 2) to take place. In the simulation section, both the ΔT^{LMA} and ΔT^{DMAC} values [i.e., (16) and (20)] obtained from Sections IV-A and B will be compared. These two values will also be verified with that acquired from the simulation results.

V. Performance Evaluation

The performance of the proposed LMA MAC algorithm is evaluated via simulations. The network simulator (ns-2, [32]) is utilized to implement the LMA MAC algorithm and to compare with other existing MAC protocols, i.e., the IEEE 802.11 and the DMAC algorithms. Two different versions of the proposed LMA MAC algorithms [i.e., the original LMA scheme and the LMA with the DB mechanism (LMA-DB)] will be evaluated. It is noted that the DMAC scheme utilized in the simulation is modified from its original version. For fair comparison, each MN will only be able to acquire its own location information. It is required for the DMAC scheme to transmit the D-RTS packets in order to obtain the location information of its neighborhood MNs. The DSR [35] protocol is adopted as the routing algorithm to perform the comparison between these MAC layer schemes.

A. Simulation Parameters

The parameters utilized in the simulations are listed as shown in Table I.

TABLE I
Simulation Parameters

Parameter Type	Parameter Value
Simulation Area	600×600 m^2
Simulation Time	800 sec
Radius of the Transmission Range with Omni Antenna	100 m
Radius of Transmission Range with Directional Antenna	200 m
Traffic Types	Constant Bit Rate (CBR)
Data Rate	200 Kbps
Size of Data Packet	1024 Bytes

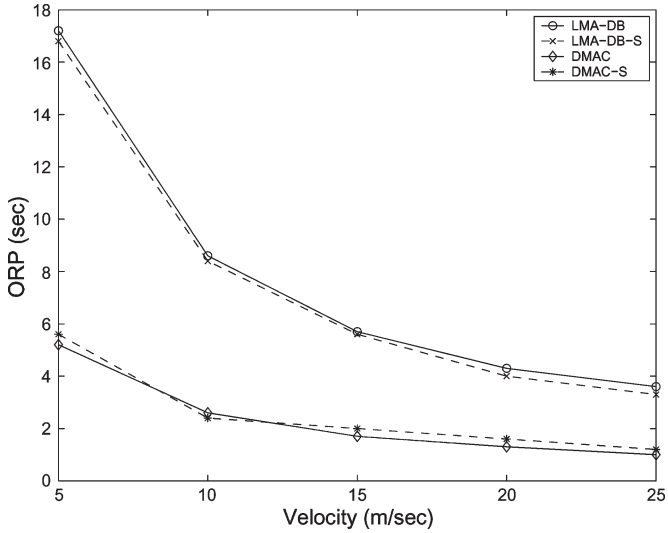

Fig. 6. Comparison of the ORP values under different velocities.

B. Simulation Results

The following metrics are utilized in the simulation for performance comparison:

1) Throughput: the total kilobit per second of data packets that are acquired by the receivers;
2) End-to-End Delay: the average time elapsed for delivering a data packet from the transmitter to the receiver;
3) Control-Packet Overhead: the ratio of the number of control packets to the number of successfully transmitted data packets.

1) Comparison Between ΔT^{LMA} and ΔT^{DMAC}: In this section, the ORP values that are computed from Section IV [i.e., ΔT^{LMA} from (16) and ΔT^{DMAC} from (20)] are validated and compared via simulations. Fig. 6 shows the comparison between the ORP values, both from the computation (i.e., LMA-DB and DMAC) and the simulation results (i.e., LMA-DB-S and DMAC-S) under different MNs' speeds. It is recognized from Section IV that both ΔT^{LMA} and ΔT^{DMAC} are functions of the relative speed V_{BA}, the relative angle α_{BA}, and the relative distance d between the two nodes A and B. In order to obtain the probabilistic effects of the ORP values, both the ΔT^{LMA} and ΔT^{DMAC} values are computed and averaged under the variations of these three parameters. The ranges of these parameters are selected as follows: $V_{BA} \sim \mathcal{N}(m, 3)$ is normally distributed, where m represents the MNs' average velocity, as considered in the x-axis of Fig. 6, $\alpha_{BA} \in [0, \pi]$,

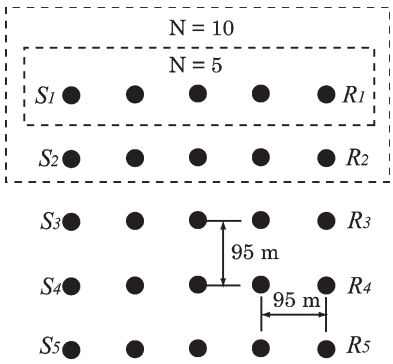

Fig. 7. Network topology with fixed MNs.

and $d \in [0, r]$, where $r = 200$ m. It is also noted that ϕ is chosen as $\pi/8$.

On the other hand, the ORP values obtained from the simulation results are conducted using the Random Waypoint Mobility (RWM) model. The RWM model is widely used to evaluate the performance of *ad hoc* protocols [36]. Each MN moves toward a randomly selected destination node with a chosen speed. The MN pauses for a preselected timeout period and resumes its movement again. The MNs' speed and timeout period are tunable parameters in order to simulate different moving environments. The simulations are performed using the proposed LMA-DB MAC and the DMAC schemes under different MN velocities. Both the time intervals ΔT^{LMA} and ΔT^{DMAC} are obtained as the averaged results from the simulations, i.e., the starting time is the time instant that two MNs exchange their location information, while the final time is acquired as the two MNs are out of the communication range with each other. As shown in Fig. 6, the ORP values obtained form both the computation and the simulation provide consistent results as expected. It is also shown that the values obtained from the LMA-DB scheme $(\Delta T^{\mathrm{LMA}})$ is comparably larger than that from the DMAC algorithm $(\Delta T^{\mathrm{DMAC}})$ under different MNs' speeds. It indicates that the communication time for two MNs is increased in the proposed LMA-DB scheme due to the location prediction and the DB mechanism. Even though the speeds go up to 25 m/s, the ΔT^{LMA} value is still around 26 ms larger than ΔT^{DMAC}.

2) Performance Comparison Under Static Networks: Fig. 7 shows the network topology with fixed MNs. The MNs, which formed a 5×5 matrix, are separated by 95 m apart between each other. The five MNs in the first column are assigned as the transmitting nodes (i.e., S_i for $i = 1, \ldots, 5$), while the MNs in the last column are the receiving nodes (i.e., R_i for $i = 1, \ldots, 5$). S_i is intended to transmit data packets to the corresponding R_i for $i = 1, \ldots, 5$. It is noted that each MN has four neighborhood MNs within its transmission range under the omnidirectional-antenna configuration. Table II illustrates the performance comparison between the proposed LMA MAC, the DMAC, and the 802.11 algorithms under the static network. Different numbers of MNs are selected in the simulation, as shown in Fig. 7. For example, the MNs in the first row are selected as $N = 5$, while the MNs in the first two rows are chosen as $N = 10$. It is also noted that the DB mechanism of the proposed LMA MAC scheme is not applied in the static-network scenario, since all the MNs are fixed without any movement.

TABLE II
PERFORMANCE COMPARISON UNDER STATIC NETWORKS (AT $V = 0$ m/s)

Number of Nodes		5	10	15	20	25
Throughput (Kbps)	LMA	191	392	560	730	735
	DMAC	190	390	520	610	615
	802.11	180	295	295	295	295
End-to-End Delay (ms)	LMA	86.0	100.0	109.9	108.0	112.0
	DMAC	90.0	104.5	114.0	115.0	120.0
	802.11	100.0	120.0	130.0	134.0	140.0
Control Packet Overhead	LMA	4.40	4.55	4.50	4.50	4.60
	DMAC	5.00	5.10	5.10	5.15	5.20
	802.11	4.50	4.60	4.60	4.60	4.70

As shown in the first item of Table II, the system throughput obtained from the LMA MAC and the DMAC schemes can achieve around 2.4 times and two times (at larger number of MNs), compared with that from the conventional 802.11 protocol. The reasons are obviously due to the following: 1) the utilization of the directional beams in these two schemes, which have twice the transmission range than the omnidirectional antennas, and 2) shorter routes for packet delivery and fewer neighborhood MNs (i.e., two neighbors) that existed using the directional beam, which results in fewer occurrences of packet collisions. Moreover, the proposed LMA MAC scheme is observed to have higher throughput (e.g., additional 120 kb/s at the number of nodes $= 25$), compared with the DMAC protocol. The major reason can be attributed to the utilization of the DLR mode in the LMA MAC scheme. With the appropriate exploitation of the DLR mechanism, the control packets are transmitted directionally from the source MN to its target MN, which results in lower probability of collision during packet transmission. On the other hand, the O-RTS packets are repeatedly transmitted within the DMAC algorithm, which can cause a comparably higher possibility for packet collision.

The second item of Table II shows the end-to-end delay comparison between these three schemes. The proposed LMA MAC scheme can achieve smaller end-to-end delay, e.g., around 10 and 30 ms fewer, compared with the DMAC and the 802.11 protocols (at the number of nodes $= 25$). The shorter delay time is obtained in the directional-antenna-based algorithms (i.e., the LMA MAC and the DMAC schemes), since only two hops are expected to transmit data packets from S_i to R_i, while four hops are required in the 802.11 protocol. Moreover, less packet collision from the LMA MAC scheme results in smaller retransmission probability and less random backoff time for contention, which causes the proposed scheme to possess shorter end-to-end delay, compared with the DMAC algorithm. The last item of Table II illustrates the comparison of the control-packet overhead between these schemes. The DMAC scheme has higher control-packet overhead comparing with the LMA MAC and the 802.11 algorithms. It is observed from the simulation that the retransmission of control packets due to the deafness problem causes excessive control overhead in the DMAC scheme. On the other hand, the proposed LMA MAC scheme utilizes the D-Listen mechanism, which can alleviate the deafness problem to some extent. The proposed scheme can provide around the same order of control-packet

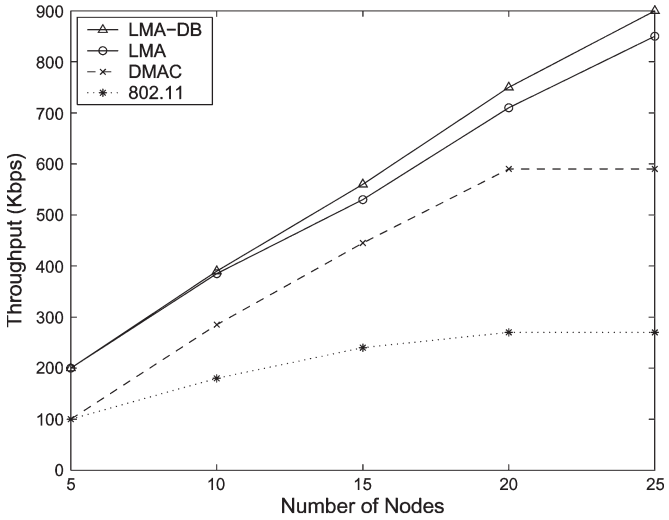

Fig. 8. Performance comparison: Throughput versus number of nodes (at $V = 10$ m/s).

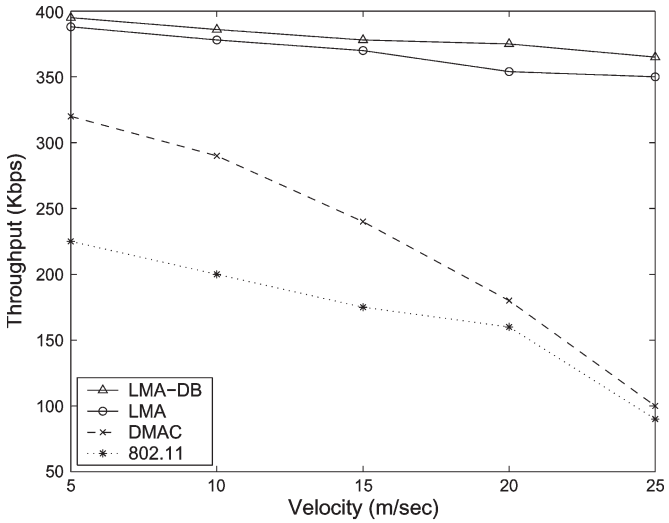

Fig. 9. Performance comparison: Throughput versus velocity (at number of Nodes $= 10$).

overhead with that obtained from the 802.11 protocol. It is noted that the deafness problem does not happen in the 802.11 protocol due to its transmission of the O-RTS/O-CTS packets.

3) Performance Comparison Under Mobile Networks: In this section, the performance comparison between the proposed LMA MAC, the DMAC, and the 802.11 protocols is conducted by considering the dynamic movements of the MNs (as shown in Figs. 8–13). The RWM model, as mentioned in Section V-B1, is adopted as the mobility model for the MNs in the simulations. It is also noted that two versions of the proposed LMA MAC algorithm are compared, i.e., the LMA scheme with and without the DB mechanism.

Figs. 8 and 9 show the throughput comparison under different number of nodes (at velocity $= 10$ m/s) and the MNs' velocities (at number of node $= 10$). With assistance from the directional antennas, the proposed LMA-DB, LMA, and the DMAC schemes possess better performance in comparison with the omnidirectional-antenna-based 802.11 protocol. Moreover, the LMA-DB MAC scheme provides the highest throughput among

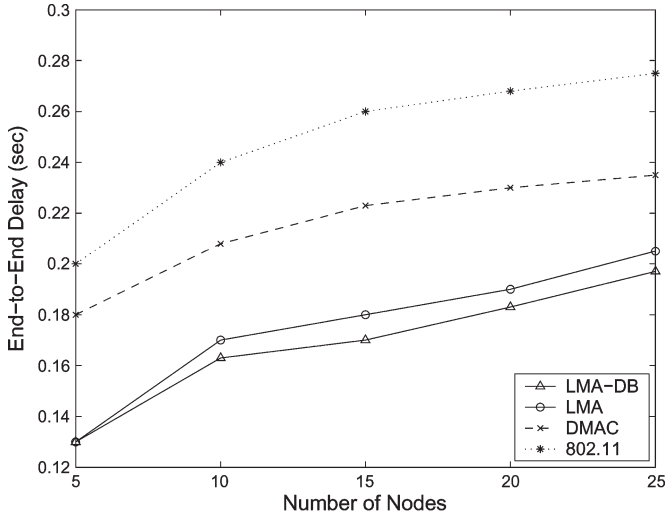

Fig. 10. Performance comparison: End-to-end delay versus number of nodes (at $V = 10$ m/s).

all the schemes under different circumstances. As shown in Fig. 8, the LMA-DB can achieve about a 3 and a 1.5 times increases of throughput (under the number of nodes $= 25$), compared with the DMAC and the 802.11 algorithms. As for the comparison between the LMA-DB and the LMA schemes, the system throughput is increased with the utilization of the DB mechanism, i.e., around a 50-kb/s increase in throughput using the LMA-DB method (at the number of nodes $= 25$). The utilization of the DBs can reduce the possibility of incorrect location prediction, while the moving behaviors of the MN are changing. As shown in Fig. 9, the prediction mechanism within the LMA-DB scheme can effectively increase the total throughput, particularly under higher moving speeds. The throughput obtained from the LMA-DB scheme is augmented for about 260 kb/s (at $V = 25$ m/s), compared with that from both the DMAC and the 802.11 protocols. It is also worthwhile to note that the throughput of the DMAC scheme decreases drastically as the MNs' moving speeds are increased. The major reason comes from the incorrect beam direction utilized in the DMAC protocol while the MNs are dynamically moving.

Figs. 10 and 11 show the comparison of the end-to-end delay under different environments. As the number of MNs is increased, the possibility of packet collision is also augmented, which results in larger end-to-end delay, as shown in Fig. 10. Compared with the 802.11 and the DMAC protocols, it can be observed that the proposed LMA-DB scheme can provide an average of 80 and 40 ms fewer in the end-to-end delay metric under different numbers of MNs. Moreover, as the speeds of the MNs are increased, as shown in Fig. 11, the end-to-end delay for all four algorithms are enlarged. With the assistance of the location prediction and the DB mechanism in the proposed LMA-DB scheme, significant reduction in the end-to-end delay can be observed, e.g., around a 220- and 180-ms decrease comparing with the 802.11 and the DMAC schemes at $V = 25$ m/s. The proposed LMA-DB scheme effectively alleviates the probability of packet collision with its prediction mechanism, such as to reduce the delay for packet delivery under various moving scenarios.

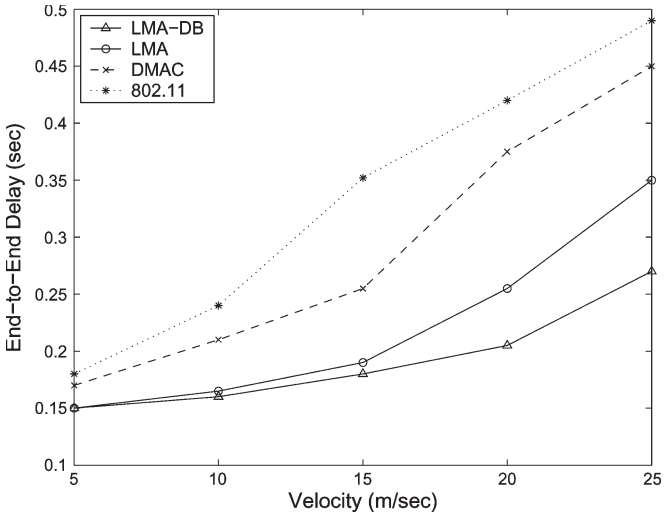

Fig. 11. Performance comparison: End-to-end delay versus velocity (at number of nodes $= 10$).

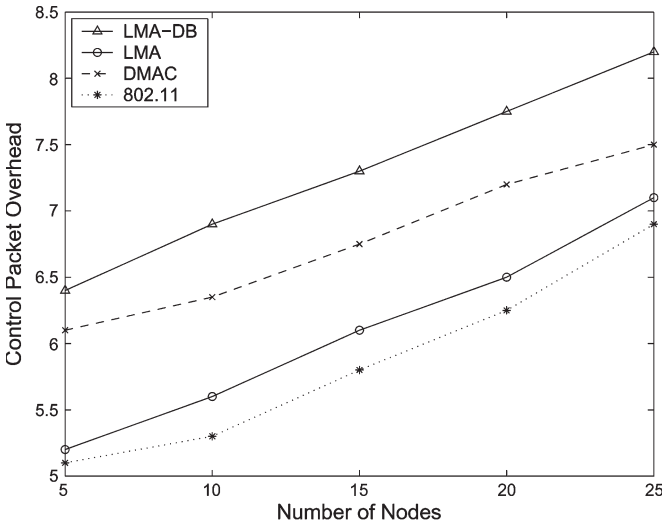

Fig. 12. Performance comparison: Control-packet overhead versus number of nodes (at $V = 10$ m/s).

Figs. 12 and 13 show the comparison of control-packet overhead under different numbers of nodes and moving speeds. As shown in Fig. 12, the LMA scheme without the DB mechanism can provide around the same order of control-packet overhead comparing with the 802.11 protocol. Without sending additional control packets, the LMA without DB scheme only attach the position-related information to its original control packets, i.e., the RTS/CTS packets. Moreover, the D-Listen mechanism reduces the possibility of packet collision. This avoids the deafness problem occurred in the DMAC algorithm, which results in comparably fewer control packets to be retransmitted between the MNs. On the other hand, the LMA-DB scheme initiates additional DB packets, while the MNs are changing their moving angles or speeds. The inevitable augmentation of the control-packet overhead within the LMA-DB scheme is observed in Fig. 12, which is served as the tradeoff for increased system throughput and smaller end-to-end delay. Fig. 13 shows the control-packet overhead under the influence of the MNs' moving speeds. As the speeds of the MNs are increased, the

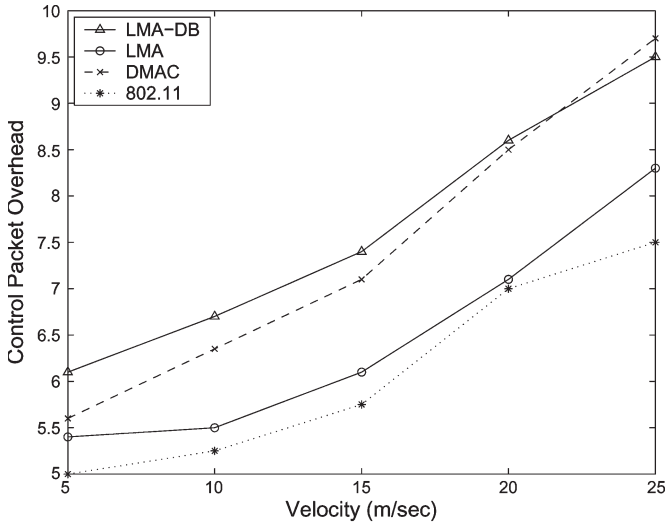

Fig. 13. Performance comparison: Control-packet overhead versus velocity (at number of nodes $= 10$).

communication linkages between the MNs are inclined to be broken. Without the location-prediction mechanism as in the LMA scheme, the DMAC algorithm continue to retransmit the control packets to facilitate the required data transmission, which results in increased control-packet overhead. Moreover, the additional control-packet overhead acquired from the LMA-DB scheme is also observed in Fig. 13 due to the additional transmission of the DBs.

Comparing with the results obtained from the static-network scenarios in the previous section, the remarkable effectiveness of the proposed LMA MAC scheme can be observed within the mobile networks. As the mobility of the MNs is increased, the proposed LMA MAC scheme (with and without the DB mechanism) can still preserve consistent system throughput and comparably smaller end-to-end delay for packet transmission. However, even with the advantages as described, there exist certain limitations while adopting the proposed LMA MAC algorithm. Considering that the MNs are continuously changing their moving directions and speeds, the performance of the LMA MAC scheme can be partially degraded. Even though the DB mechanism can alleviate the mobility-changing problem, the control overhead associated with the DBs (as shown in Figs. 12 and 13) can be augmented to some extent. As the number of DBs within the network is increased, the probability for packet collision can also be enlarged. Therefore, the proposed LMA MAC scheme is considered particularly feasible for the VANET, where the vehicles are, in general, moving at constant speeds for a certain period of time.

4) Performance Comparison Between Various Antenna Types: In this section, the influence from the various antenna types to the system performance will be investigated. As was discussed in Section III, the four categories of antenna types (as in Fig. 2) are implemented in the simulations as follows.

1) CI: The Continuous switching with Ideal antenna pattern. The spanning angle ϕ of the sector shape for the ideal antenna pattern is assigned to be $\pi/8$.
2) CR: The Continuous switching with Realistic antenna pattern. The realistic antenna pattern is designed with

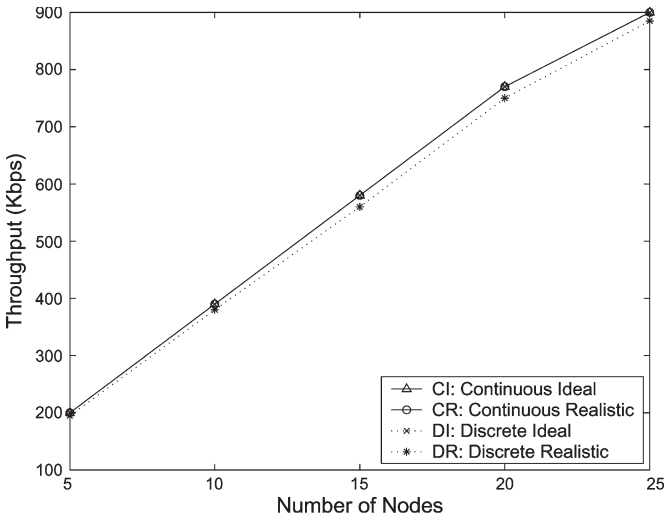

Fig. 14. Performance comparison: Throughput versus number of nodes (at $V = 10$ m/s).

spanning angle ϕ equal to $\pi/8$, where the sidelobes (defined as the $\pi/16$ along the two sides) only have 80% of the transmission power compared with that at the main lobe.

3) DI: The Discrete switching with Ideal antenna pattern. There are eight discrete antenna beams defined in the simulations, i.e., $\text{DI} = \{(\theta_i, p) | \theta_i = (2i-1)\pi/k, \theta_i \in \Re, i = 1, \ldots, k, p \in \mathcal{I}\}$ with $k = 8$. The spanning angle ϕ is also selected as $\pi/8$.
4) DR: The Discrete switching with Realistic antenna pattern. The discrete-switching mechanism is the same as that defined in case 3), while the realistic antenna pattern is the same as that in case 2).

Fig. 14 shows the throughput comparison of the four different types of antennas under different numbers of nodes. Each line is conducted using the proposed LMA-DB MAC scheme under the RWM model with the various antenna types (at $V = 10$ m/s). It can be observed in Fig. 14 that the same throughput performance is obtained from both the continuous and the discrete cases, as long as the antenna pattern is ideal, i.e., for both the CI and the DI cases. The ideal antenna pattern causes no degradation on the transmission range, no matter what type of switching mechanism is utilized. The continuous switching with realistic case (CR) can also provide almost the same throughput performance due to the continuous switching of the antenna's main lobe. As long as the location update between the MNs is frequent enough, two MNs will always be directed toward each other with their main lobe of antennas. However, the continuous-switching mechanism may require delicate antennas or excessive switching time in order to facilitate the task. On the other hand, a slightly inferior performance on the throughput is observed from the discrete switching with a realistic antenna type (DR). The reason is obvious due to the degradation of the MNs' antenna gain on the sidelobes. Two MNs that were originally in communication may fail to observe each other due to the diminished transmission ranges between the MNs.

VI. Conclusion

In this paper, a LMA MAC protocol is proposed for the directional-antenna-based VANETs. Based on the predictive location and mobility information, the MNs can effectively adjust their antenna beams in the direction of their corresponding receivers. The deafness problem can also be reduced by using the D-Listen mechanism in the proposed LMA MAC scheme. The DB associated within the proposed LMA MAC algorithm enhances the location prediction, even if the mobility of the MNs is changed during the data transmission. In order to facilitate the mechanism for location prediction, an indexing parameter, i.e., the ORP, is computed and utilized within the LMA MAC scheme. The proposed LMA MAC scheme is evaluated in simulations in comparison with the IEEE 802.11 and the DMAC protocols. The effectiveness of the proposed scheme is discussed and validated under both the static and mobile environments.

References

[1] H. Hartenstein, H. B. Fubler, and A. Festag, "FleetNet—Vehicular ad hoc network for inter-vehicle communications," in *Proc. ITS*, Nov. 2003.
[2] H. Wu, R. M. Fujimoto, R. Guensler, and M. Hunter, "MDDV: Mobility-centric data dissemination algorithm for vehicular networks," in *Proc. ACM Workshop Veh. Ad Hoc Netw.*, Oct. 2004, pp. 47–56.
[3] G. Korkmaz, E. Ekici, F. Ozguner, and U. Ozguner, "Urban multi-hop broadcast protocol for inter-vehicle communication systems," in *Proc. ACM Workshop Veh. Ad Hoc Netw.*, Oct. 2004, pp. 76–85.
[4] P. Farradyne, *Vehicle Infrastructure Integration (VII)—Architecture and Functional Requirements*. Washington, DC: Federal Highway Admin. (FHWA), Apr. 2005. Draft Version 1.0.
[5] J. Blum, A. Eskandarian, and L. J. Hoffman, "Challenges of intervehicle ad hoc networks," *IEEE Trans. Intell. Transp. Syst.*, vol. 5, no. 4, pp. 347–351, Dec. 2004.
[6] *Wireless LAN Medium Access Control (MAC) and Physical Layer (PHY) Specifications*, 1997. IEEE Std. 802.11.
[7] J. Zander, "Slotted ALOHA multihop packet radio networks with directional antennas," *Electron. Lett.*, vol. 26, no. 25, pp. 2098–2100, Dec. 1990.
[8] T. S. Yum and K. W. Hung, "Design algorithms for multihop packet radio networks with multiple directional antennas stations," *IEEE Trans. Commun.*, vol. 40, no. 11, pp. 1716–1724, Nov. 1992.
[9] H. Singh and S. Singh, "DOA-ALOHA: Slotted ALOHA for ad hoc networking using smart antennas," in *Proc. IEEE VTC—Fall*, Oct. 2003, pp. 2804–2808.
[10] Z. Huang and C.-C. Shen, "A comparison study of omnidirectional and directional MAC protocols for ad hoc networks," in *Proc. IEEE Globecom*, Nov. 2002, pp. 57–61.
[11] B. Parkinson and S. Gilbert, "NAVSTAR: Global positioning system—Ten years later," *Proc. IEEE*, vol. 71, no. 10, pp. 1177–1186, Oct. 1983.
[12] A. Acampora and S. Krishnamurthy, "A new adaptive MAC layer protocol for broadband packet wireless networks in harsh fading and interference environments," *IEEE/ACM Trans. Netw.*, vol. 8, no. 3, pp. 328–336, Jun. 2000.
[13] A. Chandra, V. Gummalla, and J. Limb, "Wireless medium access control protocols," *Commun. Surveys Tuts.*, vol. 3, no. 2, pp. 2–15, 2000.
[14] Y. Ko, V. Shankarkumar, and N. Vaidya, "Medium access control protocols using directional antennas in ad hoc networks," in *Proc. IEEE INFOCOM*, Tel Aviv, Israel, Mar. 2000, vol. 1, pp. 13–21. (3).
[15] A. Nasipuri, S. Ye, J. You, and R. E. Hiromoto, "A MAC protocol for mobile ad hoc networks using directional antennas," in *Proc. IEEE WCNC*, Chicago, IL, Sep. 2000, pp. 1214–1219.
[16] Y. Wang and J. J. Garcia-Luna-Aceves, "Spatial reuse and collision avoidance in ad hoc networks with directional antennas," in *Proc. IEEE Globecom*, Nov. 2002, pp. 112–116.
[17] S. Bandyopadhyay, K. Hausike, S. Horisawa, and S. Tawara, "An adaptive MAC and directional routing protocol for ad hoc wireless networks using ESPAR antenna," in *Proc. ACM/SIGMOBILE MobiHoc*, Oct. 2001, pp. 243–246.

[18] R. R. Choudhury, X. Yang, R. Ramanathan, and N. H. Vaidya, "Using directional antennas for medium access control in ad hoc networks," in *Proc. ACM MobiCom*, Sep. 2002, pp. 59–70.
[19] P. Karn, "MACA—A new channel access method for packet radio," in *Proc. 9th Comput. Netw. Conf.*, 1990, pp. 134–140.
[20] R. Ramanathan, "On the performance of ad hoc networks with beamforming antennas," in *Proc. ACM MobiHoc*, Oct. 2001, pp. 95–105.
[21] T. Korakis, G. Jakllari, and L. Tassiulas, "A MAC protocol for full exploitation of directional antennas in ad-hoc wireless networks," in *Proc. ACM MobiHoc*, Jun. 2003, pp. 98–107.
[22] Z. Haas and J. Deng, "Dual busy tone multiple access (DBTMA)—A multiple access control scheme for ad hoc networks," *IEEE Trans. Commun.*, vol. 50, no. 6, pp. 975–985, Jun. 2002.
[23] Z. Huang, C. Shen, C. Srisathapornphat, and C. Jaikaeo, "A busy-tone based directional MAC protocol for ad hoc networks," in *Proc. IEEE MILCOM*, Anaheim, CA, Oct. 2002, pp. 1233–1238.
[24] H. Gossain, C. Cordeiro, D. Cavalcanti, and D. P. Agrawal, "The deafness problems and solutions in wireless ad hoc networks using directional antennas," in *Proc. IEEE Globecom*, Anaheim, CA, Nov. 2004, pp. 108–113.
[25] R. R. Choudhury and N. H. Vaidya, "Deafness: A MAC problem in ad hoc networks when using directional antennas," in *Proc. 12th IEEE ICNP*, 2004, pp. 283–292.
[26] K. Nagashima, M. Takata, and T. Watanabe, "Evaluations of a directional MAC protocol for ad hoc networks," in *Proc. 24th ICDCSW*, 2004, pp. 678–683.
[27] M. Sekido, M. Takata, M. Bandai, and T. Watanabe, "Directional NAV indicators and orthogonal routing for smart antenna based ad hoc networks," in *Proc. 25th IEEE ICDCSW*, Jun. 2005, pp. 871–877.
[28] M. Takai, J. Martin, A. Ren, and R. Bagrodia, "Directional virtual carrier sensing for directional antennas in mobile ad hoc networks," in *Proc. ACM MobiHoc*, Jun. 2002, pp. 183–193.
[29] Y. Li and A. M. Safwat, "DMAC-DACA: Enabling efficient medium access for wireless ad hoc networks with directional antennas," in *Proc. 1st Int. Symp. Wireless Pervasive Comput.*, Jan. 2006, pp. 1–5.
[30] S. Bellofiore, J. Foutz, R. Govindarajula, I. Bahceci, C. A. Balanis, A. S. Spanias, J. M. Capone, and T. M. Duman, "Smart antenna system analysis, integration and performance for mobile ad-hoc networks (MANETs)," *IEEE Trans. Antennas Propag.*, vol. 50, no. 5, pp. 571–581, May 2002.
[31] A. Arora and M. Krunz, "Interference-limited MAC protocol for MANETs with directional antennas," in *Proc. 6th IEEE Int. Symp. World Wireless Mobile Multimedia Netw.*, Jun. 2005, pp. 2–10.
[32] J. C. Liberti and T. S. Rappaport, *Smart Antennas for Wireless Communications: IS-95 and Third Generation CDMA Applications*. Englewood Cliffs, NJ: Prentice-Hall, 1999.
[33] P. H. Lehne and M. Pettersen, "An overview of smart antenna technology for mobile communications systems," *Commun. Surveys Tuts.*, vol. 2, no. 4, pp. 2–13, 1999.
[34] J. Heidemann, N. Bulusu, J. Elson, C. Intanagonwiwak, K. Lan, Y. Xu, W. Ye, D. Estrin, and R. Govindan, "Effects of detail in wireless network simulation," in *Proc. SCS Multiconference Distrib. Simul.*, Jan. 2001, pp. 3–11.
[35] D. B. Johnson, D. A. Maltz, and J. Broch, "DSR: The dynamic source routing protocol for multi-hop wireless ad hoc networks," in *Ad Hoc Networking*, C. E. Perkins, Ed. Reading, MA: Addison-Wesley, 2001.
[36] X. Hong, M. Gerla, G. Pei, and C. Chiang, "A group mobility model for ad hoc wireless networks," in *Proc. ACM Int. Workshop Model. Simul. Wireless Mobile Syst.*, Aug. 1999, pp. 53–60.

Kai-Ten Feng (M'03) was born in Taipei, Taiwan, R.O.C., in 1970. He received the B.S. degree from the National Taiwan University, Taipei, in 1992, the M.S. degree from the University of Michigan, Ann Arbor, in 1996, and the Ph.D. degree from the University of California, Berkeley, in 2000.

He was with the OnStar Corporation, a subsidiary of General Motors Corporation, as an In-Vehicle Development Manager/Senior Technologist between 2000 and 2003. His major responsibilities with OnStar include the design of future telematics platforms and in-vehicle networks. Since February 2003, he has been with the Department of Communication Engineering, National Chiao Tung University, Hsinchu, Taiwan, as an Assistant Professor. His current research interests include mobile *ad hoc* networks, wireless-sensor networks, embedded system design, wireless-location technologies, and intelligent transportation systems.

Dr. Feng was the recipient of the Best Paper Award from the IEEE Vehicular Technology Conference (VTC) Spring 2006, which was ranked as the first among the 615 accepted papers. He has served on the technical program committees of VTC, the Asia Pacific Wireless Communications Symposium, and the International Conference on Communications, Circuits, and Systems.